Neuroscience 311 (2015) 153–165

EVENT-RELATED BRAIN POTENTIALS DURING THE VISUOMOTOR MENTAL ROTATION TASK: THE CONTINGENT NEGATIVE VARIATION SCALES TO ANGLE OF ROTATION

M. HEATH, [a,b]* **C. D. HASSALL,** [c] **S. MACLEAN** [d] **AND O. E. KRIGOLSON** [c,e]

[a] *School of Kinesiology, University of Western Ontario, London, ON, Canada*

[b] *Graduate Program in Neuroscience, University of Western Ontario, London, ON, Canada*

[c] *Faculty of Education, University of Victoria, Victoria, BC, Canada*

[d] *Department of Psychology and Neuroscience, Dalhousie University, Halifax, NS, Canada*

[e] *Division of Medical Sciences, University of Victoria, Victoria, BC, Canada*

Abstract—Perceptual judgments about the angular disparity of a character from its standard upright (i.e., mental rotation task) result in a concurrent increase in reaction time (RT) and modulation of the amplitude of the P300 event-related brain potential (ERP). It has therefore been proposed that the P300 represents the neural processes associated with a *visual* rotation. In turn, the visuomotor mental rotation (VMR) task requires reaching to a location that deviates from a target by a predetermined angle. Although the VMR task exhibits a linear increase in RT with increasing oblique angles of rotation, work has not examined whether the task is supported via a visual rotation analogous to its mental rotation task counterpart. This represents a notable issue because seminal work involving non-human primates has ascribed VMR performance to the motor-related rotation of directionally tuned neurons in the primary motor cortex. Here we examined the concurrent behavioral and ERP characteristics of a standard reaching task and VMR tasks of 35°, 70°, and 105° of rotation. Results showed that the P300 amplitude was larger for the standard compared to each VMR task – an effect independent of the angle of rotation. In turn, the amplitude of the contingent negative variation (CNV) – an ERP related to cognitive and visuomotor integration for movement preparation – was systematically modulated with angle of rotation. Thus, we propose that the CNV represents an ERP correlate related to the cognitive and/or visuomotor transformation demands of increasing the angular separation between a stimulus and a movement goal.

Key words: action, event-related brain potential, contingent negative variation, reaching, movement, visuomotor mental rotation.

INTRODUCTION

When we reach to touch an icon on a computer tablet the spatial overlap between the icon and the endpoint for the reaching response permits the evocation of maximally effective and efficient motor output (henceforth referred to as standard task: see Fitts and Seeger, 1953). The optimized performance of standard tasks reflects their mediation via visuomotor networks residing in the dorsal visual pathway that operate largely independent of top-down (i.e., cognitive) control (Goodale, 2011). It is, however, important to recognize that the spatial relations between a stimulus and a response (SR) can be flexibly decoupled allowing an individual to complete their movement to a location that deviates from the stimulus (henceforth referred to as non-standard task). As a real world example of this issue, a novice performer must understand that anterior-posterior movement of their finger on a computer trackpad leads to up-down movement of a cursor appearing on the computer's screen. Thus, non-standard tasks represent an important line of inquiry because they provide a framework to understand the neural mechanisms related to the top-down control of actions (Rossetti et al., 2005) and the early learning of novel SR mappings (Fitts and Seeger, 1953).

The visuomotor mental rotation (VMR) task is an example of a non-standard task and requires that performers complete a center-out reaching movement to a location that deviates from a visual target by a predetermined angle. A consistent finding from the VMR literature is that reaction time (RT) for *oblique* angles increase linearly with increasing angle of rotation (Georgopoulos and Massey, 1987; Pellizzer and Georgopoulos, 1993; Neely and Heath, 2010a, 2011; for saccades see Fischer et al., 1999)[1]. Moreover, single-cell recording work in non-human primates has shown that

*Correspondence to: M. Heath, School of Kinesiology and Graduate Program in Neuroscience, University of Western Ontario, London, ON N6A 3K7, Canada. Tel: +1-519-661-2111x80498.
E-mail address: mheath2@uwo.ca (M. Heath).

Abbreviations: CNV, contingent negative variation; EEG, electroencephalography; ERP, event-related brain potential; MD, movement direction; PPC, posterior parietal cortex; RT, reaction time; rTMS, repetitive transcranial magnetic stimulation; SR, spatial relations between a stimulus and a response; VMR, visuomotor mental rotation.

[1] The VMR task produces RTs that systematically increase with increasing oblique angles, however, RTs for the cardinal axes (i.e., 90° and 180°) do not give rise to a linear rise in RT. In particular, 90° and 180° (also referred to as antipointing) VMR tasks results in shorter RTs than intermediary angles of 5° or greater (Neely and Heath, 2010a, 2011). The basis for this effect is that familiarity with cardinal angles results in a movement planning process that does not require the systematic rotation of a movement vector.

http://dx.doi.org/10.1016/j.neuroscience.2015.10.018
0306-4522/

VMR responses are associated with the analog rotation of directionally tuned motor cortical neurons from the location of the target to the instructed response location (Georgopoulos et al., 1989). As such, Georgopolous et al. assert that VMR planning times are defined by the temporal costs associated with the *motor-related* rotation of a movement vector (i.e., the mental rotation model: MRM; for a review see Georgopoulos and Pellizzer, 1995).

A limitation of the current VMR literature is the paucity of work examining the neural mechanisms associated with task performance in humans. Of course, we recognize that an extensive literature has examined the electroencephalographic properties of the mental rotation task (MR) (for a review see Heil, 2002). Notably, the MR task requires the classification of a character (i.e., letter or number) presented in different orientations and results have shown a linear increase in RT as a function of the character's angular disparity from a 'standard' upright position (Cooper and Shepard, 1973; see also Shepard and Metzler, 1971). What is more, the amplitude of the P300 event-related brain potential (ERP) is systematically modulated as a function of the character's angular disparity (Peronnet and Farah, 1989; Wijers et al., 1989; Heil, 2002; Milivojevic et al., 2009). More specifically, the P300 amplitude becomes increasingly negative with increasing rotation. The P300 is identified as a parieto-central positive deflection in the electroencephalography (EEG) with a peak 250–500-ms post stimulus onset (for a review see Polich, 2007). Moreover, one interpretation of the waveform is that it reflects the revision of a 'mental model' when a mismatch exists between a stimulus and a required response (i.e., context-updating) (Donchin and Coles, 1988; Nieuwenhuis et al., 2005). As such, modulation of the P300 in the MR task may reflect the demands of rotating a stimulus until it matches the performer's mental model (i.e., the character's standard upright position). It is, however, important to recognize that the MR task differs from the VMR task in at least three important respects. First, the MR task does not entail a goal-directed response and is therefore not constrained by speed-accuracy relations in movement planning (for a review see Elliott et al., 2011). Second, the MR task does not require the transformation of visual coordinates into a motor response (i.e., visuomotor transformation). Third, the MR task requires obligatory classification of the presented character, whereas no such classification is required for the VMR task. Thus, it remains unclear as to whether the electroencephalographic correlates of the VMR task correspond to their MR counterparts.

To our knowledge Bestmann et al.'s (2002) repetitive transcranial magnetic stimulation (rTMS) study represents the only work to examine the cortical areas involved in the VMR task in human participants. In that study, participants completed standard (0°) and VMR (35°, 70°, 105°, and 140°) tasks in conditions wherein rTMS was applied to the left and right posterior parietal cortex (PPC) and the vertex (i.e., the control condition) during response planning. Results showed that RTs were longer when rTMS was applied to the left or right PPC for the extreme angles of rotation (i.e., 105° and 140°). The authors proposed that the PPC supports the top-down coupling between the process of rotation and the required motor output. Although Bestmann et al's findings provide an initial understanding of the neural mechanisms supporting the VMR task, their work was not designed to identify a psychophysiological marker for the task's onset. Moreover, there is no electroencephalographic or neuroimaging evidence from humans examining whether the VMR task is selectively related to: (1) the motor-related rotation of a movement vector (i.e., the MRM model), (2) an early visual rotation akin to that reported in the MR literature (i.e., P300 scaling to angle of rotation), and (3) the cognitive and/or visuomotor demands associated with increasing the angular separation between a stimulus and an intended motor goal. Indeed, in the latter case it may be that the concurrent cognitive *and* visuomotor demands of the VMR task render a movement planning process that is entirely distinct from the visual rotation supporting the MR task. As such, the contingent negative variation (CNV) may be sensitive to the cognitive and visuomotor demands supporting the VMR task. The CNV was first identified by Walter et al. (1964) and reflects an early frontocentral and a later centroparietal component that comprise a sustained negativity during the preparation period of a goal-defined action. The early and late components are thought to respectively represent the orienting properties of a stimulus (Loveless and Sanford, 1974) and the cognitive and visuomotor properties that support response preparation (Brunia, 1988; see also Zaepffel and Brochier, 2012). Further, the component originates in cognitive, visuomotor and motor structures (i.e., M1, supplementary motor area, premotor area and parietal cortex) (see Lamarche et al., 1995; Bares et al., 2007) linked to the preparation of standard and non-standard reaching movements (Connolly et al., 2000). As such, the CNV represents a candidate ERP component to index the cognitive and/or visuomotor demands of an upcoming response (for a review see Gómez and Flores, 2011).

The present study examined the ERPs associated with the VMR task wherein participants were provided advanced information regarding the nature of an upcoming response (i.e., 0°, 35°, 70° and 105°). For each trial, a single target was presented and EEG data were time-locked to its onset. Notably, and in contrast to previous VMR studies, the onset of the target stimulus did not serve as the movement imperative (see Georgopoulos and Massey, 1987; Heath et al., 2009; Neely and Heath, 2009, 2010a,b, 2011; Maraj and Heath, 2010); rather, responses were cued between 900 and 1100 ms following target onset. Such a methodology was used to: (1) dissociate the ERPs associated with movement planning (e.g., P300) from those associated with movement execution (i.e., the Bereitschaftspotential)[2], and (2) accurately identify onset of the neural processes associated with the VMR task. In terms of research predictions, if the VMR task is selectively mediated via a motor-related rotation than neither the P300 nor the

[2] The late CNV and Bereitschaftspotential share many common neural generators; however, the late CNV differs importantly from the Bereitschaftspotential in terms of its modulation by non-motoric factors such as task difficulty (Bajric et al., 1999) and sensorimotor demands (Brunia, 1988).

CNV amplitude should systematically scale to the angle of rotation. In turn, if the VMR task is, in part, supported via an early visual rotation of a target's spatial location then the amplitude of the P300 should systematically vary with the angle of rotation. Of course, such a finding in combination with the extant MR literature would provide convergent evidence of an electroencephalographic marker for the top-down demands of an early visual rotation. Last, if concurrent cognitive and visuomotor processes engender distinct movement preparation demands then the CNV should systematically vary with angle of rotation.

EXPERIMENTAL PROCEDURES

Participants

Twenty self-declared right-handed participants (age range: 18–33 years; 12 female) with normal or corrected-to-normal vision and no history of a neurological or psychiatric disorder volunteered for this study. Participants signed consent forms approved by the local research ethics board and this work was conducted according to the ethical standards laid down in the Declaration of Helsinki.

Apparatus and procedures

Participants sat for the duration of the experiment in front of a tabletop (770 mm in height) and completed center-out reaching movements with their right hand to target stimuli appearing on a 26-inch (576 mm by 323 mm) touchscreen monitor (60 Hz, 8-ms response rate, 800 by 600 pixels, Elo Touch Solutions IntelliTouch 2639L, Milpitas, CA, USA). The monitor was placed at the participants' midline and 50 mm from the front edge of the tabletop. Visual stimuli were set against a high-contrast gray background and included: (1) an unfilled black square (16 mm by 16 mm) located at the monitor's center which served as the limb's start location and the gaze fixation location, and (2) filled black target squares (11 mm by 11 mm) positioned at 45° increments around an imaginary concentric circle surrounding the start location. The eccentricity from the start/fixation location to a target was 133 mm. Experimental events were controlled via MATLAB (8.2, MathWorks; Natick, MA, USA) and the Psychophysics Toolbox extensions (ver 3.1: Brainard, 1997).

The start of a testing session began with a general instruction screen indicating that participants would complete separate blocks of trials involving standard (i.e., 0°) and VMR (35°, 70° and 105°) reaching movements. The general instruction screen indicated that rotations in the VMR blocks should be completed in a clockwise direction from the target stimulus (Neely and Heath, 2010a, 2011; see also Georgopoulos and Massey, 1987). As well, participants were instructed to maintain their gaze at the start/fixation location until the end of a trial. The fixation instruction was used to reduce oculomotor-related EEG artifacts and a chin rest was used to restrict head movements. Following the general instruction screen, participants were provided a 'block' instruction screen that indicated the requirements for the upcoming series of trials. For example, the instruction screen for 35° angle of rotation stated: ''*In the next block of trials, you will complete a series of reaching responses that are rotated 35 degrees (in the clockwise direction) from the target stimulus. The line drawing below represents an angle of 35 degrees. Remember to fixate the small square in the center of your visual field for the duration of the trial. Please complete your response as quickly and accurately as possible*". The aforementioned line drawing was a pictorial representation wherein the origin was centered on the monitor (see Fig. 1 for angle-specific line drawing examples). The block instruction screen was available in advance of each block and participants could view the screen (and associated pictorial representation) for as long as they wished. Once the participant indicated that they were comfortable with the block instruction screen it was extinguished and was not viewed again.

As shown in Fig. 1, a trial began with the projection of the start/fixation location that cued participants to place their right forefinger on its location. Following contact with the touchscreen a randomized foreperiod was introduced (500 to 700 ms) after which one of the eight targets was presented for the duration of the trial. After a delay of 900–1100 ms, a 50-ms tone (3000 Hz sine wave) cued participants to complete their reaching response. In contrast to previous work (i.e., Georgopoulos and Massey, 1987; Neely and Heath, 2010a, 2011), the onset of the target stimulus did not serve as the response imperative; rather, we included the 900–1100-ms interval between target onset and response cuing to dissociate the ERPs associated with movement planning (e.g., P300) from those associated with movement execution (i.e., the Bereitschaftspotential). Each angle of rotation block included six randomly ordered trials to each of the different target locations (i.e., 48 trials/block) and each block was repeated on three occasions (i.e., 576 total experimental trials). The ordering of the different blocks was randomized.

EEG recording

Prior to data collection participants were fitted with an active Ag/AgCl 64-electrode EEG cap. The electrodes were mounted in the standard 10–20 layout and were recorded using BrainVision PyCorder software (Version 1.0.4, Brainproducts GmbH, Munich, Germany) with a virtual ground built into the amplifier (reference-free acquisition). Electrooculograms were obtained by electrodes placed above and below the right eye and on the outer canthi of the left and right eyes. Electrical impedances for all electrodes were kept below 20 kΩ at all times. EEG data were sampled at 500 Hz, amplified (ActiCHamp, Version 2, Brainproducts GmbH, Munich, Germany) and filtered through an anti-aliasing low-pass filter of 8 kHz.

Dependent variables

The touchscreen display had a contact spatial resolution of 0.53 mm and a sampling frequency of 56 Hz. RT was the time between the auditory cue and release of

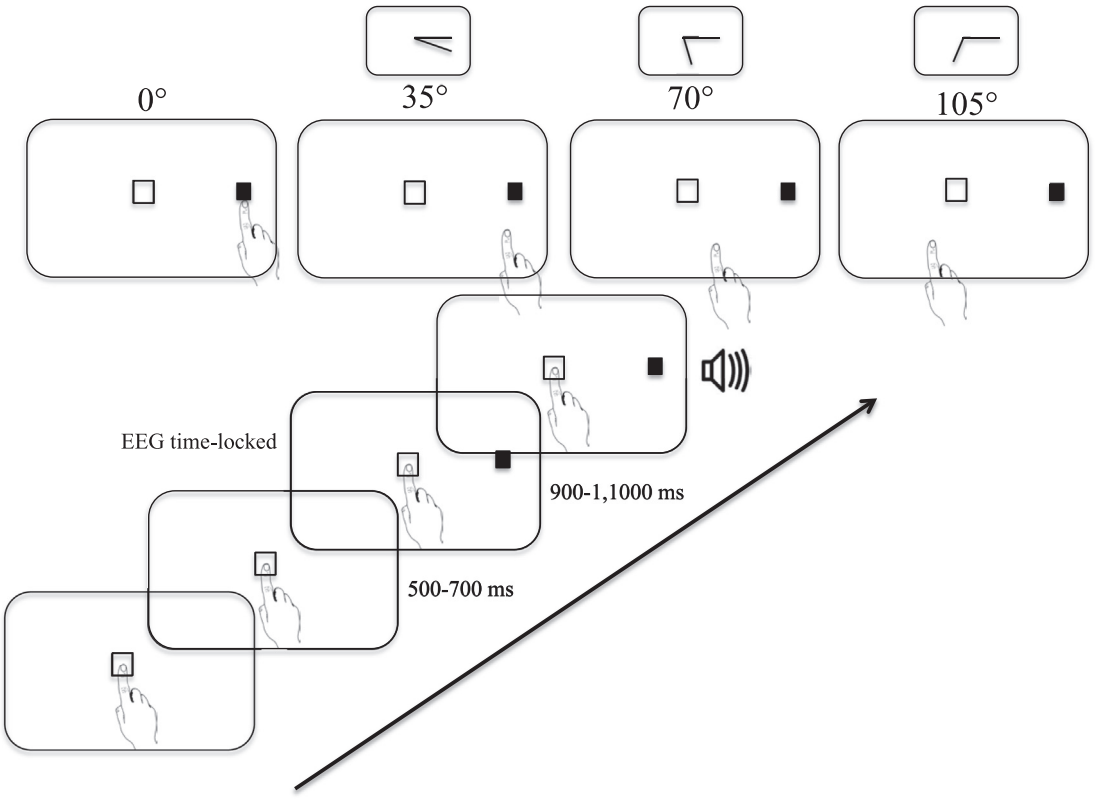

Fig. 1. Timeline of visual-, auditory- and movement-related events. A central square served as the start/fixation location and contact of the forefinger with this position initiated a trial sequence. In particular, following contact a 500–700-ms interval was initiated after which time one of eight targets was presented. For simplicity, the figure displays only one target (i.e., black filled square). EEG data were time-locked to target onset and a tone presented 900–1100 ms post target onset served as the movement imperative. The top panels show the relative position of the hand at movement offset for the standard (i.e., 0°) and VMR tasks (i.e., 35°, 70°, and 105°). Participants were instructed to maintain their gaze on the start/fixation location for the duration of a trial to avoid ocular-related artifacts (see also Neely and Heath, 2010a). Last, the smaller panels above the numerical label for each VMR condition represents the pictorial line drawing provided in each instruction block screen.

contact from the touchscreen (i.e., < 85 g of contact force with the touchscreen). The end of a reaching movement was determined when greater than 85 g of contact force was applied to the touchscreen. Movement direction (MD; i.e., systematic endpoint error) was computed as the angle between the required and achieved movement endpoint. For example, MD values of 358° and 2° represent responses that were respectively 2° counterclockwise and clockwise to the direction of the required response. As such, we computed MD via standard circular statistics techniques (Batschelet, 1981) using the CircStat toolbox for MATLAB (Berens, 2009). In addition, we computed the within-participants variability of MD using standard circular statistics techniques. Last, we computed the constant error of radial distance (in mm) to determine whether participants' reaches under – (negative valence) or overshot (positive valence) the required movement amplitude.

The EEG was recorded and pre-processed in a manner identical to Krigolson et al. (2008, 2012). To analyze the visual response to target onset, ERP waveforms were created by averaging epochs of the pre-processed data spanning from 200 ms before target onset to 1000 ms after target onset from the continuous EEG data separately for each angle of rotation block. We did not separately analyze reaches to each target location due to an insufficient number of trials (i.e., 18 trials per target per condition). Based on previous literature (N100 see Luck and Hillyard, 1995; P300 see Donchin and Coles, 1988; CNV see Loveless and Sanford, 1974) and concomitant visual inspection of the grand average ERP waveforms and ERP component topographies we observed three components of interest over occipital, parietal and central electrode sites. Specifically, we observed: (1) modulation of the N100 at electrodes O1 and O2, (2) modulation of the P300 at electrode Pz, and (3) modulation of the CNV at electrode Cz. For the purposes of statistical analysis, we quantified each ERP component as the mean voltage for each participant ± *x* ms of the maximal difference in the grand average waveforms at the channel where the effect was most prominent (*x* reflects an estimate of the window needed to capture component width derived from visual inspection). Thus, the N100 was quantified as the mean voltage ± 10 ms of the peak (~200 ms) on channels O1 and 02; the P300 as the mean voltage ± 25 ms of the peak (~325 ms) on channel Pz; and the CNV as the mean voltage ± 50 ms of the peak (~550 ms) on channel Cz for each experimental condition for each participant.

Statistical analyses

RT data were excluded if values were less than 150 ms or greater than two standard deviations above a participant-specific mean (Neely and Heath, 2010a). Independent component analysis was used to remove EEG artifacts related to eye blinks, and gradient and absolute amplitude differences were used within an artifact rejection algorithm to remove trials involving smooth or saccadic eye movements. Trials were also removed from the epoched EEG data for gradient artifacts (10 uV/ms) and/or maximum to minimum restrictions – a change of more than 100 uV within any given epoch. Some of the exclusion criteria overlapped and only those trials involving a valid RT and EEG signal were analyzed: less than 12% of trials for any participant were removed from our final data analyses. Dependent variables were examined via one-way (i.e., angle of rotation: 0°, 35°, 70°, 105°) repeated measures ANOVA. Where appropriate, *F*-ratios were adjusted for violations of sphericity using the appropriate Huynh–Feldt correction (corrected degrees of freedom reported to one decimal place). Significant main effects were decomposed via power-polynomials (i.e., trend analyses: Pedhazur, 1997). Further, we report partial eta-squared (η_p^2) and eta-squared (η^2) statistics to facilitate comparison to the extant literature and to support the practical significance of the current findings (Lakens, 2013)[3].

RESULTS

Behavioral data

Fig. 2 shows that RTs increased systematically with increasing angle of rotation, $F(3,57) = 25.66$, $p < 0.001$, $\eta_p^2 = 0.57$, $\eta^2 = 0.27$ (only linear effect significant: $F(1,19) = 36.57$, $p < 0.001$). Recall that unlike previous work (Georgopoulos and Massey, 1987; Neely and Heath, 2010a, 2011), responses were cued 900–1100 ms following target onset. Hence, the systematic modulation of RTs indicates that the angle-specific planning process continued up to and after response cuing.

Fig. 3 provides polar histograms of trial-to-trial achieved angles for all participants and shows that average MD values scaled in relation to the requirements of each rotation condition, $F(1.0,20.1) > 3000$, $p < 0.001$; $\eta_p^2 = 0.98$, $\eta^2 = 0.97$ (only linear effect significant: $F(1,19) > 12{,}000$, $p < 0.001$) (see also Fig. 2). In other words, the direction of participants' responses was commensurate with task instructions. To determine if the different angles of rotation exhibited a systematic bias we contrasted MD values for each angle of rotation to their veridical instruction angle (i.e., 0°, 35°, 70° and 105°) via single-sample *t*-tests. Results showed that MD values for each angle of rotation did not reliably differ from veridical (all $t(19) < 1$ for the 0°, 35°, and 70° angles of rotation, and $t(19) = 1.43$, $p = 0.17$ for the 105° angle of rotation, all $d_z < 0.15$). As such, the different conditions did not produce systematic counter- or clockwise rotation errors. Notably, however, the polar histograms show that trial-to-trial MD variability increased with increasing angle of rotation, $F(1.3,26.1) = 18.57$, $p < 0.001$, $\eta_p^2 = 0.49$, $\eta^2 = 0.29$ (only linear effect significant: $F(1,19) = 21.56$, $p < 0.001$). Further, constant error associated with radial distance was influence by angle of rotation, $F(2.0,38.6) = 44.10$, $p < 0.001$, $\eta_p^2 = 0.77$, $\eta^2 = 0.46$, and demonstrated an increased undershooting bias with increasing angle of rotation (significant linear effect: $F(1,19) = 59.33$, $p < 0.001$: 0° = −9 mm, SD = 6; 35° = −24 mm, SD = 12, 70° = 35 mm, SD = −20; 105° = −40 mm, SD = 22). Thus, although participants directed their response to an appropriate goal location (i.e., MD data), results for MD variability and constant error in radial distance indicated that endpoint precision decreased with increasing angle of rotation (see also Fig. 2).

ERP data

Fig. 4 presents grand-average ERP waveforms for each angle of rotation across a subset of electrode sites when time-locked to target onset. The figure qualitatively demonstrates the electrode sites associated with maximal differences between our components of interest. In term of our quantitative analyses, Fig. 5 shows component-specific waveforms for each angle of rotation when time-locked to target onset for an average of channels O1 and O2. The figure demonstrates that the N100 produced a reliable effect of angle of rotation, $F(3,57) = 4.33$, $p < 0.01$, $\eta_p^2 = 0.19$, $\eta^2 = 0.03$, such that the amplitude decreased (i.e., became more positive) from the 0° to the 35° condition and then plateaued (i.e., 35° = 70° = 105°: significant quadratic polynomial: $F(1,19) = 5.27$, $p < 0.04$). Fig. 6 presents ERP waveforms for channel Pz highlighting the P300 effect we observed – the component produced a reliable effect of angle of rotation, $F(3,57) = 6.45$, $p < 0.001$, $\eta_p^2 = 0.25$, $\eta^2 = 0.08$. Specifically, the P300 amplitude decreased from the 0° to the 35° angle of rotation (i.e., become more negative) and then plateaued (i.e., 35° = 70° = 105°: significant quadratic polynomial: $F(1,19) = 13.69$, $p < 0.01$). In other words, the P300 differentiated *between* standard and VMR tasks but not *within* the different angles of rotation.

Fig. 7 shows ERP waveforms for channel Cz. The figure demonstrates that the CNV was systematically modulated by angle of rotation, $F(3,57) = 12.92$, $p < 0.001$, $\eta_p^2 = 0.40$, $\eta^2 = 0.17$: the component became less negative with increasing angle of rotation (significant linear polynomial: $F(1,19) = 33.54$, $p < 0.001$). Moreover, Fig. 7 qualitatively shows that the waveform separation between angle of rotation conditions (i.e., linear scaling with increasing rotation) was sustained up to 1000-ms post-target onset – a result consistent with the view that the late component of the CNV represents a sustained negativity recorded during the preparatory period of a response (Walter et al., 1964).

[3] One-way repeated measures ANOVAs employ common formulae for the computation of eta-squared and generalized eta-squared statistics (Bakeman, 2005).

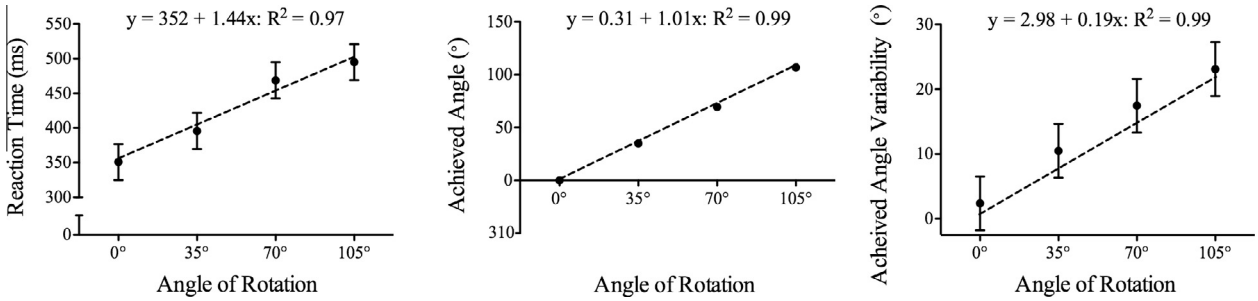

Fig. 2. Mean reaction time (ms), achieved angle (MD: °) and achieved angle variability (°) for each angle of rotation. Error bars represent 95% within-participant confidence intervals computed via the mean-squared error term from the ANOVA model (Loftus and Masson, 1994). For the MD data the size of the confidence intervals are less than the width of the symbols depicting the mean values and are therefore not visible. In all panels the hatched line represents the linear regression of each variable to the angle of rotation and the associated regression equation is presented at the top of each panel (Note: for the MD panel the regression line overlaps with the identify line representing the veridical location for each angle of rotation). Further, simple effects contrasts between the 0° and 35°, 35° and 70°, and 70° and 105° angles of rotation across reaction time (all $t(19) > 4.42$, all $p < 0.001$), MD (all $t(19) > 19.56$, all $p < 0.001$) and achieved angle variability (all $t(19) > 2.31$, all $p < 0.04$) were significant – a finding underscoring the power-polynomial approach in the Results asserting that values for all variables increased with increasing angle of rotation.

Correlation of CNV amplitude to RT and constant error of radial distance

For each angle of rotation we computed correlation coefficients relating CNV amplitude to RT and constant error of radial distance. Results indicated that CNV amplitude was neither related to RT (all $r < 0.37$, all $p > 0.11$) nor constant error of radial distance (all $r < 0.19$, all $p > 0.42$). Thus, results indicate that *within* each angle of rotation condition CNV amplitude was independent of movement planning time and the amplitude of the reaching response.

DISCUSSION

We examined the concurrent behavioral and ERP components of standard (i.e., 0°) and VMR (35°, 70°, and 105°) reaching movements. In particular, electroencephalographic data were used to determine whether reaching to an area dissociated from a visual target is supported via a visual rotation (i.e., the P300) and/or represents the concurrent cognitive and visuomotor demands of transforming a target's spatial location (i.e., the CNV).

Behavioral measures: Increasing angle of rotation diminishes the efficiency and effectiveness of response planning and execution

In the classic VMR task the onset of a target serves as the movement imperative and RTs in this paradigm increase linearly with increasing oblique angles of rotation (e.g., Georgopoulos and Massey, 1987; Neely and Heath, 2010a, 2011). In turn, the present investigation cued responses 900–1100 ms following target onset – an event-related design used to disentangle the ERP component(s) associated with movement planning from movement execution (i.e., the Bereitschaftspotential) (see Heath et al., 2012). Given this manipulation, we predicted that angle-specific computational processes would have been completed by the time of response cuing and thereby rendered equivalent RTs for standard and VMR tasks. In contrast to that prediction, a systematic increase in RT was associated with increasing angle of rotation. Thus, a tentative conclusion drawn from our RT data is that the VMR task is entirely subserved via the motor-related rotation of a movement vector and is a process that occurs only after response cuing (i.e., the MRM hypothesis). Notably, however, we contrasted RTs from the present study to an earlier investigation employing the same angles of rotation as used here but in a classic VMR cuing paradigm (Neely and Heath, 2010a). *A posteriori* analysis indicated that RTs in the present study were on average 147 ms less than the matched angles of rotation used by Neely and Heath (all $t(28) > 5.23$, all $p < 0.001$ for each matched VMR angle). In other words, the cuing condition employed here produced a large RT reduction. This finding in combination with the ERP results described below (see *The CNV scales to angle of rotation*) indicate that participants were engaged in angle-specific movement planning processes prior to response cuing.

The results for achieved endpoints demonstrated that participants' responses scaled in relation to the different angles of rotation, and neither the standard nor the VMR tasks were associated with a systematic rotation bias (i.e., counter- or clockwise rotation bias). In terms of endpoint variability, the standard task was less variable than each VMR task – a result attributed to the fact that direct SR mapping enables the specification of motor output via the absolute visuomotor networks of the dorsal visual pathway (Goodale, 2011). As well, endpoint variability increased systematically with angle of rotation and constant error for radial distance indicated an increased undershooting bias with increasing angle of rotation. As reported previously (Neely and Heath, 2010a, 2011), such a result is attributed to the 'cost' of SR decoupling and the increased noise associated with the rotation of a target's spatial position over increasing angles. Taken together then, our behavioral results demonstrate that increasing oblique angles of rotation produced longer RTs and diminished the effectiveness of movement execution.

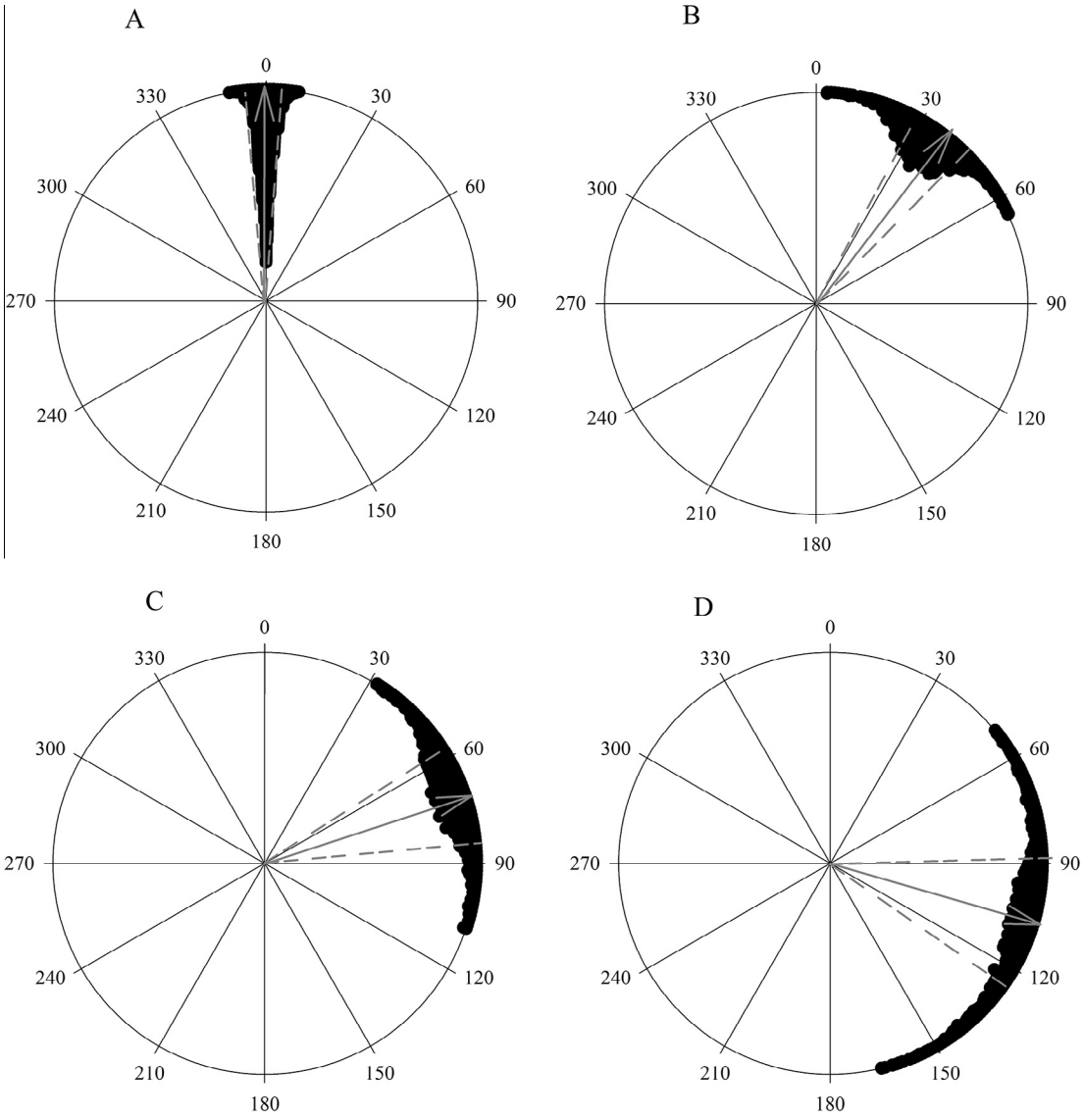

Fig. 3. Polar histograms representing the achieved angle (i.e., the angle between the instructed and the achieved endpoint) for the 0° (A), 35° (B), 70° (C) and 105° (D) angle of rotation blocks. Bins widths are 1° and the degree of stacking at each bin represents an increased frequency. The location of the target stimulus has been normalized to 0° and the arrow represents the mean achieved angle for all trials (i.e., MD: see *Data collection, dependent variables and statistical analyses*), whereas the hatched lines represent one circular standard deviation.

The N100: Differences between standard and VMR tasks are independent of angle of rotation

The visual N100 is observed at inferoposterior and anterosuperior electrode sites that peak 150 to 200 ms after the abrupt onset of a visual stimulus (for a review see Hopfinger et al., 2004)[4]. For example, a left- or rightward arrow precue provided in advance of the presentation of a left or right visual field target results in shorter RTs and a larger N100 amplitude when the precue and the target are directionally congruent than when incongruent (e.g., Harter et al., 1989). The increased N100 amplitude in such a context has been linked to a neural analog for enhanced attention in a restricted area of visual space (Hopfinger et al., 2004; see also Mangun, 1995). Recall, however, that the present investigation did not provide a precue related to target location, and targets were randomly presented at one of eight locations (i.e., as opposed to being restricted left and right of fixation). As such, participants were not able to predict the location of an upcoming target and were therefore required to adopt a distributed attentional strategy to reflect the multiple target locations used here. For that reason, we did not *a priori* identify the N100 as a component of interest. That said, visual inspection of the EEG data showed that the N100 amplitude for the standard task was larger (i.e., more negative) than the VMR tasks (which did not differ) at inferoposterior electrode sites (i.e., O1 and O2) with a peak deflection in the component's identified latency window (i.e., 200-ms post target onset). In

[4] In the present study the N100 refers to the visual N100 component as opposed to the auditory N100 component (for a recent review of this issue see Joos et al., 2014). As well, research has not clearly identified the relationship between N100 discrimination and spatial attention effects (Vogel and Luck, 2000).

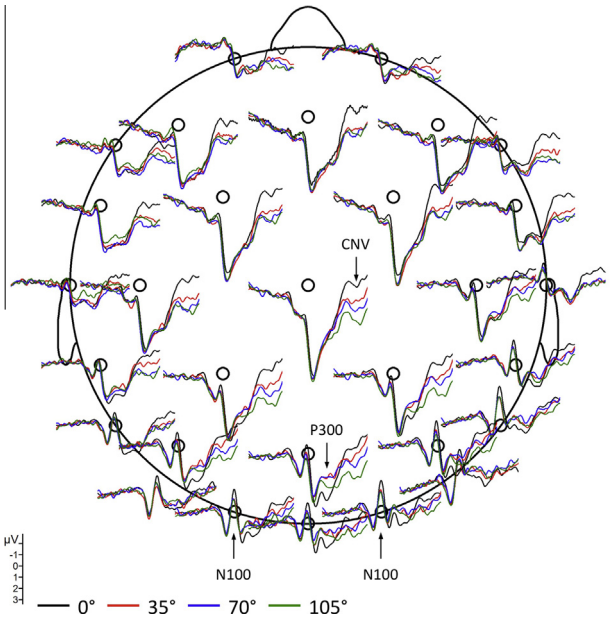

Fig. 4. Grand-average event-related brain potential waveforms (uV) for a broad subset of electrode sites as a function of angle of rotation when time-locked to target onset.

accounting for this finding we recognize that the N100 reflects not only the focus of attention but is also modulated when participants are performing a discrimination task. For example, the N100 is larger for a choice-RT as compared to a simple-RT task (Ritter et al., 1983; Vogel and Luck, 2000). Accordingly, Vogel and Luck proposed that the increased amplitude for the choice-RT task reflects a general neural substrate for the ‘‘operation of a visual discrimination mechanism” (p. 202). Although Vogel and Luck employed the term ‘discrimination’ to broadly reflect discriminating between multiple stimuli we believe that such an explanation provides a parsimonious account for the present investigation. More specifically, we propose that the larger N100 associated with the standard task reflects enhanced discrimination between initial limb position and target location; after all, the target’s veridical location in this task serves as the goal for the ensuing response. As such, the direct SR mapping associated with a standard task may support enhanced discrimination of the egocentric coordinates necessary for a successful response. In turn, the smaller amplitude for the VMR tasks is taken as evidence of reduced discrimination processes to facilitate SR decoupling. Put more simply, the VMR task requires spreading attentional and discrimination mechanisms between the limb and the: (1) veridical target location, and (2) the required endpoint associated with the rotation response. In support of our view, Doran and Hoffman (2010) found that the N100 was reduced when discriminating between target and distractors – a result taken to evince that a distractor requires the deployment of discrimination mechanisms to multiple stimulus locations (see also Bettencourt and Somers, 2009). Although we recognize that our proposal awaits further evaluation, we believe that the present results add importantly to the movement neuroscience and the general ERP literature for two reasons. First, results show that SR decoupling is associated with an early difference in movement planning and is unrelated to the degree of visual rotation. Second, our findings demonstrate that the N100 *may* represent a reliable metric for dissociating the visually based demands of goal-directed reaching.

An issue that requires addressing is whether the shorter RTs in the standard task influenced ERP activity

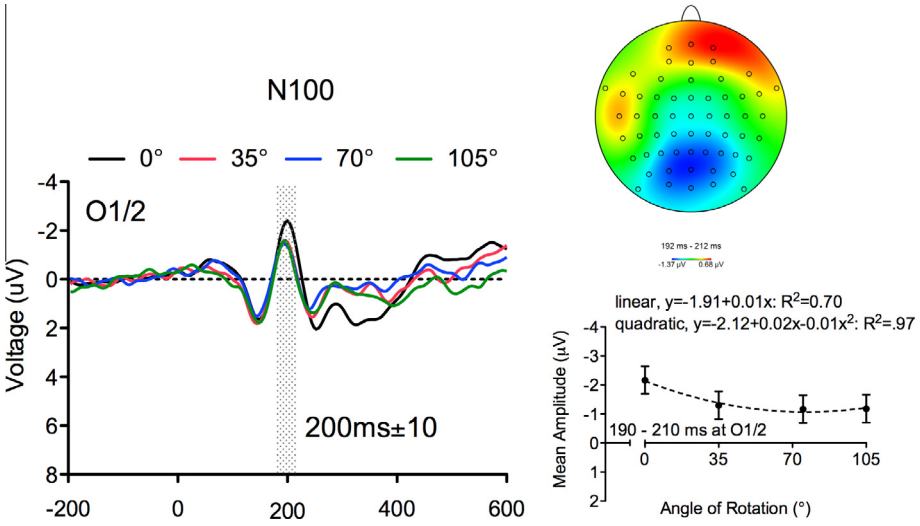

Fig. 5. The main panel depicts grand average event-related brain potential waveforms (uV) at averaged occipital electrode sites (O1 and O2). The smaller offset figures show scalp topographies and mean voltages for each angle of rotation (i.e., the amplitude of the N100). The offset figure providing the mean N100 amplitude includes the quadratic regression line and reports the associated regression equation and R^2 value. Additionally, we report the linear regression equation (and associated R^2 value) to demonstrate that hierarchical analysis showed that the quadratic polynomial produced a reliable increase in the proportion of explained variance ($p < 0.01$). Error bars represent the 95% within-participant confidence interval computed via the mean-squared error term from the ANOVA model (Loftus and Masson, 1994). Further, and in complement to the power-polynomial presented in the Results, simple effects contrasts indicated that the amplitude of the N100 decreased from the 0° to 35° angle of rotation ($t(19) = 3.00$, $p < 0.01$), but did not reliably vary between the 35° and 70°, and 70° and 105° angles of rotation (all $t(19) < 1$).

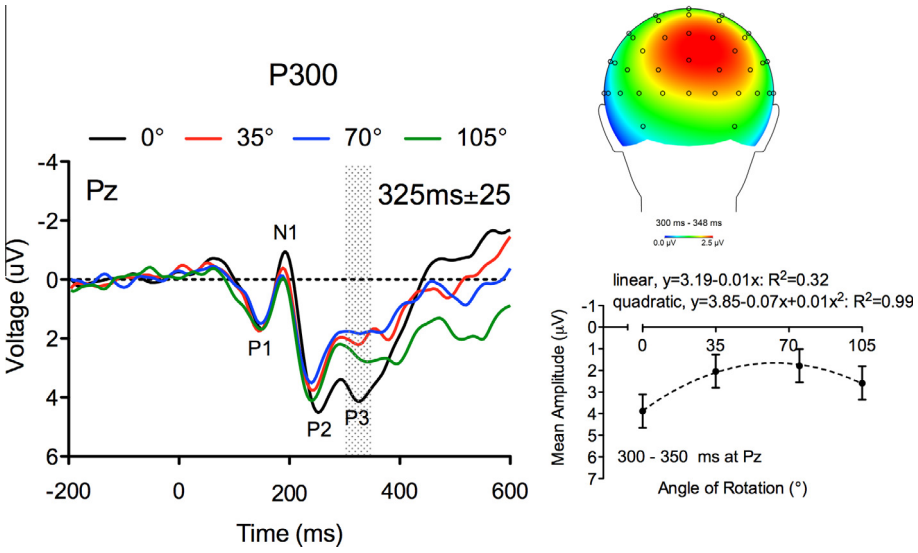

Fig. 6. The main panel depicts grand average event-related brain potential waveforms (uV) at parietal electrode site Pz when time-locked to target onset for each angle of rotation (i.e., 0°, 35°, 70°, 105°). The smaller offset figures show scalp topographies and mean voltages for each angle of rotation (i.e., the amplitude of the P300). The offset figure providing the mean P300 amplitude includes the quadratic regression line and regression equation and additionally reports the linear regression equation. We report both linear and quadratic regression equations (and associated R^2 values) to demonstrate that hierarchical analysis showed that the former produced a reliable increase in the proportion of explained variance ($p < 0.001$). Further, and in complement to the power-polynomial presented in the Section Results, simple effects contrasts showed that the amplitude of the P300 decreased from the 0° to 35° angle of rotation, $t(19) = 3.28$, $p < 0.01$), but did vary between the 35° and 70° ($t(19) < 1$), and the 70° and 105°, $t(19) = 1.60$, $p = 0.13$, angles of rotation. Error bars as per the conventions outlined in Fig. 5.

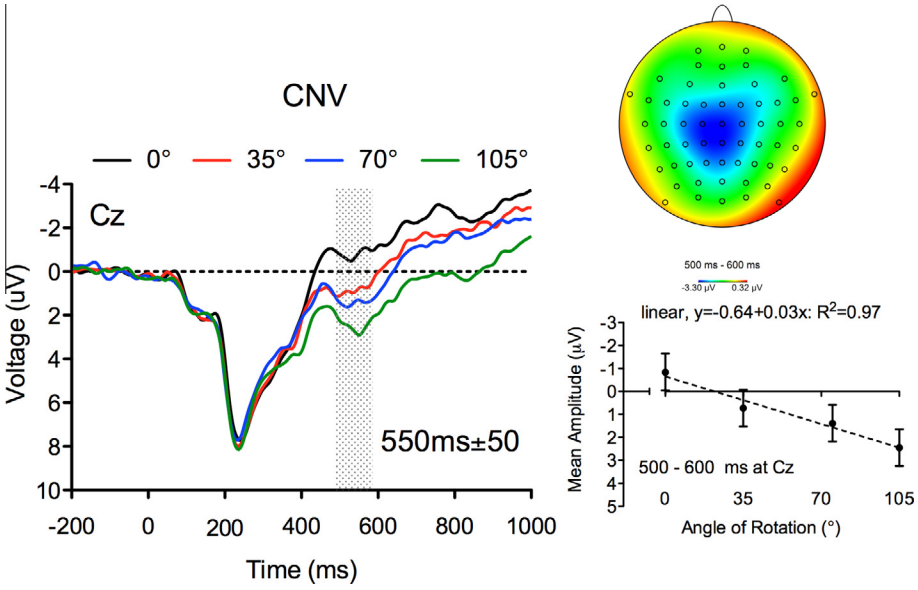

Fig. 7. The main panel depicts grand average event-related brain potential waveforms (uV) at central electrode site Cz when time-locked to target onset for each angle of rotation (i.e., 0°, 35°, 70°, 105°). The smaller offset figures show scalp topographies and mean voltages for each angle of rotation (i.e., the amplitude of the CNV) and their associated linear regression line and regression equation. Further, and in complement to the power-polynomial presented in the Results, simple effects contrasts indicated that the amplitude of the CNV became less negative across the 0° and 35°, 35° and 70°, and 70° and 105° angles of rotation (all $ts(19) > 2.94$, all $p < 0.01$). Error bars as per the conventions outlined in Fig. 5.

in the time frame of the N100 (see Kutas and Donchin, 1980). In addressing this issue we emphasize that EEG data were time locked to target onset, and responses were subsequently cued 900–1100 ms thereafter. Thus, the interval between target presentation and response cuing in combination with the average RT of the standard and VMR tasks (i.e., average = 427 ms; see Fig. 2) indicates that the N100 modulation is unrelated to between-task differences in premotor activity.

The P300: No evidence for a visual rotation

The MR literature reports that the P300 amplitude becomes increasingly negative with increasing angle of

rotation (Peronnet and Farah, 1989; Wijers et al., 1989; Heil, 2002; Milivojevic et al., 2009). Wijers et al. proposed that this result reflects a slow parietal negativity wave imposed on the simultaneously occurring P300 and that the increased negativity reflects the concurrent activity of occipital and parietal structures in visual rotation. Moreover, Wijers et al. and Heil (2002) assert that the P300 modulation represents direct electrophysiological evidence of a visual rotation. In the present investigation the P300 amplitude for the standard task was larger than the VMR tasks – which did not differ (i.e., 35° = 70° = 105°). In other words, the P300 did not demonstrate an analog process of visual rotation. Instead, the difference between the standard and VMR tasks is consistent with a number of goal-directed movement studies demonstrating that the P300 indexes a task-set required to decouple SR relations (Krigolson et al., 2008; Heath et al., 2012; Kang et al., 2014; Weiler and Heath, 2014; for a review of context-updating hypothesis see Donchin and Coles, 1988). For example, Krigolson et al. reported that online trajectory corrections related to an unexpected target 'jump' were preceded by a modulation of the P300 amplitude, and Weiler et al. reported a P300 modulation for oculomotor responses requiring SR decoupling (i.e., pro-versus anti-saccade) (see also Kang et al., 2014). Accordingly, we propose that the P300 difference observed here reflects that the VMR tasks require a cognitively demanding task-set supporting SR decoupling.

We were somewhat surprised that the P300 did not scale to angle of rotation in a manner commensurate to the MR literature. Of course, one possible reason for this discrepancy is that our task required that participants complete their reaching response 900–1100 ms following target onset, whereas the MR task typically requires an obligatory perceptual response immediately after stimulus onset (Peronnet and Farah, 1989; Wijers et al., 1989; Heil, 2002; Milivojevic et al., 2009). It is, however, important to recognize that some work has shown that the process of mental rotation begins immediately after stimulus presentation and occurs even when a delay is introduced between stimulus presentation and the onset of an overt response (Richter et al., 1997; Hyun and Luck, 2007; Volcic et al., 2010; Christophel et al., 2015). Furthermore, single-cell recording in the parietal lobe (i.e., lateral intraparietal cortex) of non-human primates has shown that a visual and motor transformation process occurs during the memory interval of a delayed antisaccade task (Zhang and Barash, 2000; see also Heath et al., 2012). Thus, that the present experiment did not observe a systematic scaling of the P300 to angle of rotation is not likely attributed to use of a 'delayed' VMR paradigm because the MR literature (and work from the antisaccade task) ascribes visual rotation as continuous in nature. An alternative explanation for the discrepant P300 findings is that the MR task requires the active classification of a character's identify and the rotation of the character about its axis until it is aligned with a standard upright. In contrast, top-down identification is not required for the VMR task; rather, participants must decouple SR relations and implement a movement in peripersonal space that deviates from the cued target location. This is a salient difference because the constituent elements of the MR task have been linked to a visual rotation within an allocentric (i.e., scene-based) frame of reference, whereas the demands of the VMR task mandate sensorimotor transformations within an egocentric frame of reference (see Asakura and Inui, 2011). Thus, that the P300 amplitude in our VMR task did not systematically scale to angle of rotation may reflect that the frame of reference (i.e., egocentric) and associated neural mechanisms (i.e., duplex model of visual processing; for an extensive review see Goodale, 2011) underlying the task are distinct from those mediating the MR task. In further support for this position, MR and VMR tasks elicit a salient difference in their respective RTs. In particular, Wijers et al. and Heil (see also Milivojevic et al., 2009) reported that MR tasks including angles up to 180° demonstrate a linear increase in RT, whereas VMR tasks involving 90° and 180° angles always produce RTs that are less than their oblique counterparts (i.e., including angles as small as 5°: see Neely and Heath, 2010a, 2011). Accordingly, it has been proposed that familiarity with cardinal axes (the oblique effect: see Howe and Purves, 2005) precludes the need for a time-consuming visual rotation and results in a direct vector inversion. Thus, coalescent behavioral and electroencephalographic evidence demonstrate that the visuomotor transformations underlying the VMR task are distinct from the more 'cognitive' and visual nature of the MR task.

The CNV scales to angle of rotation

As noted in the Introduction, the CNV is thought to reflect the cognitive and visuomotor properties that contribute to stimulus orientation and movement preparation (Brunia, 1988). Moreover, a number of studies report that CNV amplitude increases and RT decreases with the amount of advanced information associated with a motor response (Leuthold et al., 1996; Ulrich et al., 1998) – a finding interpreted to reflect that movement planning is associated with discrete stages of information processing (i.e., dual process theory of motor preparation: see Jentzsch et al., 2004). The present study observed that the CNV amplitude systematically decreased with increasing angle of rotation, and was inversely related to RT. For example, the standard task was associated with the largest CNV amplitude and shortest RT, whereas the 105° VMR task was associated the smallest CNV amplitude and longest RT. As such, one possible explanation for the present findings is that the direct SR relationship associated with a standard task permitted a more complete movement preparation process. In turn, the linear decrease in CNV amplitude – and associated inverse relationship with RT – may reflect the serial cognitive and visuomotor processes associated with angle-specific computational demands. This view is compatible with evidence showing that cognitive effort (Ulrich et al., 1998) and/or the evaluation of task difficulty (Bajric et al., 1999) required in a forthcoming response modulated CNV amplitude. A second, and not mutually exclusive, explanation is that the VMR task does not

entail an explicit 'visual' rotation but rather a 'visuomotor' rotation during the early and late stages of movement preparation. In support of this position, the cortical generators of the CNV (primary motor cortex, supplementary motor area, premotor area, parietal cortex) (see Bares et al., 2007) comprise a frontoparietal network that is known to support the visuomotor transformations of standard and non-standard (i.e., antipointing and antisaccade) saccades and reaching movements (Connolly et al., 2000; Herweg et al., 2014; see also Zhang and Barash, 2000; Moon et al., 2007). Thus, the angle-specific modulation of the CNV observed here might reflect a visuomotor transformation between the observed stimulus and the intended movement goal. Of course, we recognize that the above-mentioned proposals are speculative and await further evaluation. That being said, our results provide the first demonstration of an electroencephalographic correlate of the VMR task, and demonstrate that the neural processes associated with the VMR task are distinct from its MR counterpart.

Two final issues require addressing: The first relates to reconciling our results with Georgopoulos et al.'s (1989) observation that a motor-related rotation of a movement vector supports the VMR task. In addressing this issue, we in no way contend that the present findings negate those of Georgopolous et al; rather, we believe that our results are complementary and suggest that the cognitive and visuomotor demands of dissociating a stimulus from an intended movement goal may sequentially support the motor-related rotation of a movement vector. Further, and although the present study was not designed to disentangle the putative cognitive-, visuomotor- and motor-related contributions to the VMR task, it is possible that each contributes to a neural loop supporting the transformations necessary for effective reaching (Fortier et al., 1993). Future EEG work may seek to more directly examine this issue via independent component analysis (ICA) of EEG and a concomitant *measure projection analysis* of ICA signals. In particular, a recent study by Ofori et al. (2015) showed that such an approach serves to identify the cortical regions supporting the distinct stages (i.e., ballistic vs. deceleration) of goal-directed reaching movements. Thus, a three-dimensional EEG approach may serve to localize the distinct cognitive-, visuomotor-, and cognitive-related processes associated with the constituent elements of the VMR task. The second issue to address is whether ERPs associated with motor preparation or motor execution were modulated by the angle of rotation. To address that issue, Fig. 8 presents supplementary data showing the amplitude of the readiness (RP) and Bereitschaftspotential (BP) potentials (i.e., EEG time-locked to movement onset) as a function of each angle of rotation. Results showed that the BP amplitude did not vary with angle of rotation, $F < 1$. In turn, the RP amplitude showed a reliable effect of angle of rotation, $F(3,57) = 7.07$, $p < 0.01$, $\eta_p^2 = 0.27$, such that the amplitude became more negative from the 0° to the 35° angle of rotation and then plateaued (35° = 70° = 105°) (i.e., significant quadratic polynomial: $F(1,19) = 6.46$, $p < 0.03$). As noted in previous work by our group (Krigolson et al., 2012), the RP effect likely

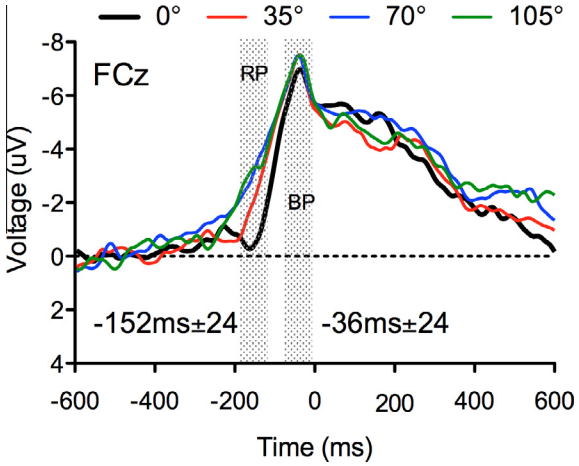

Fig. 8. Grand average event-related brain potential waveforms (uV) at channel FCz when time-locked to movement onset for each angle of rotation (i.e., 0°, 35°, 70°, 105°). The figure shows ERPs for the readiness (RP) and Bereitschaftspotential (BP) potentials. The RP amplitude was quantified as the mean voltage ±24 ms of the peak (~−152 ms), and the BP was quantified at as the mean voltage ±24 ms of the peak (~−36 ms) (see Luck, 2014). Notably, the figure demonstrates that neither RP nor BP amplitudes were systematically modulated by angle of rotation.

reflects that endpoints in the VMR tasks were associated with greater undershooting error than the standard condition (*see constant error of radial distance*). Of course, what is most notable is that neither motor preparation (i.e., RP) nor execution (i.e., BP) processes were *systematically* influenced by the angle of rotation manipulation used here. As such, our supplemental analyses provide further evidence that the CNV represents the ERP correlate associated with the visuomotor and/or cognitive demands of the VMR task.

CONCLUSIONS

The present findings provide the first examination of the electroencephalographic correlates of the VMR task. In particular, we propose that the CNV represents the ERP correlate of the cognitive and visuomotor demands associated with performing a VMR task over increasing angular separation between a stimulus and the intended location of a reaching response.

Acknowledgments—Supported by a Discovery Grant from the Natural Sciences and Engineering Research Council of Canada and Major Academic Development Fund and Faculty Scholar Awards from the University of Western Ontario. We declare no commercial, financial or other conflict of interest.

REFERENCES

Asakura N, Inui T (2011) Disambiguation of mental rotation by spatial frames of reference. i-Perception 2:477–485.

Bajric J, Rösler F, Heil M, Hennighausen E (1999) On separating processes of event categorization, task preparation, and mental rotation proper in a handedness recognition task. Psychophysiology 36:399–408.

Bakeman R (2005) Recommended effect size statistics for repeated measures designs. Behav Res Methods 37:379–384.
Batschelet E (1981) Circular statistics in biology. London: Academic Press.
Berens P (2009) CircStat: a MATLAB toolbox for circular statistics. J Stat Softw 31:1–21.
Bares M, Nestrasil I, Rektor I (2007) The effect of response type (motor output versus mental counting) on the intracerebral distribution of the slow cortical potentials in an externally cued (CNV) paradigm. Brain Res Bull 71:428–435.
Bestmann S, Thilo KV, Sauner D, Siebner HR, Rothwell JC (2002) Parietal magnetic stimulation delays visuomotor mental rotation at increased processing demands. NeuroImage 17:1512–1520.
Bettencourt KC, Somers DC (2009) Effects of target enhancement and distractor suppression on multiple object tracking capacity. J Vis 9:9.
Brainard DH (1997) The psychophysics toolbox. Spat Vis 10:433–436.
Brunia CH (1988) Movement and stimulus preceding negativity. Biol Psychol 26:165–178.
Christophel TB, Cichy RM, Hebart MN, Haynes JD (2015) Parietal and early visual cortices encode working memory content across mental transformations. Neuroimage 106:198–206.
Connolly JD, Goodale MA, Desouza JF, Menon RS, Vilis T (2000) A comparison of frontoparietal fMRI activation during anti-saccades and anti-pointing. J Neurophysiol 84:1645–1655.
Cooper LA, Shepard RN (1973) Chronometric studies of the rotation of mental images. In: Chase G, editor. Visual information processing. New York: Academic Press. p. 72–121.
Donchin E, Coles MG (1988) Is the P300 component a manifestation of context updating? Behav Brain Sci 11:357–374.
Doran MM, Hoffman JE (2010) Target enhancement and distractor suppression in multiple object tracking. Visual Cogn 18:126–129.
Elliott D, Helsen WF, Chua R (2011) A century later: Woodworth's (1899) two-component model of goal-directed aiming. Psychol Bull 127:342–357.
Fischer MH, Deubel H, Wohlschläger A, Schneider WX (1999) Visuomotor mental rotation of saccade direction. Exp Brain Res 127:224–232.
Fitts PM, Seeger CM (1953) S-R compatibility: spatial characteristics of stimulus and response codes. J Exp Psychol 46:199–210.
Fortier PA, Smith AM, Kalaska JF (1993) Comparison of cerebellar and motor cortex activity during reaching: directional tuning and response variability. J Neurophysiol 69:1136–1149.
Georgopoulos AP, Massey JT (1987) Cognitive spatial-motor processes. 1. The making of movements at various angles from a stimulus direction. Exp Brain Res 65:361–370.
Georgopoulos AP, Lurito JT, Petrides M, Schwartz AB, Massey JT (1989) Mental rotation of the neuronal population vector. Science 243:234–236.
Georgopoulos AP, Pellizzer G (1995) The mental and the neural: psychological and neural studies of mental rotation and memory scanning. Neuropsychologia 33:1531–1547.
Gómez CM, Flores A (2011) A neurophysiological evaluation of a cognitive cycle in humans. Neurosci Biobehav Rev 35:452–461.
Goodale MA (2011) Transforming vision into action. Vision Res 51:1567–1587.
Harter MR, Miller SL, Price NJ, LaLonde ME, Keyes AL (1989) Neural processes involved in directing attention. J Cogn Neurosci 1:223–237.
Heath M, Bell J, Holroyd CB, Krigolson O (2012) Electroencephalographic evidence of vector inversion in antipointing. Exp Brain Res 221:19–26.
Heath M, Maraj A, Gradkowski A, Binsted G (2009) Anti-pointing is mediated by a perceptual bias of target location in left and right visual space. Exp Brain Res 192:275–286.
Heil M (2002) The functional significance of ERP effects during mental rotation. Psychophysiology 39:535–545.
Herweg NA, Weber B, Kasparbauer A, Meyhöfer I, Steffens M, Smyrnis N, Ettinger U (2014) Functional magnetic resonance imaging of sensorimotor transformations in saccades and antisaccades. Neuroimage 102(Pt 2):848–860.
Hopfinger JB, Luck SJ, Hillyard SA (2004) Selective attention: electrophysiological and neuromagnetic studies. In: Gazzniga M, editor. The cognitive neurosciences. Cambridge: The MIT Press. p. 561–574.
Howe CQ, Purves D (2005) Natural-scene geometry predicts the perception of angles and line orientation. Proc Natl Acad Sci U S A 102:1228–1233.
Hyun J-S, Luck SJ (2007) Visual working memory as the substrate for mental rotation. Psychon Bull Rev 14:154–158.
Jentzsch I, Leuthold H, Richard Ridderinkhof K (2004) Beneficial effects of ambiguous precues: parallel motor preparation or reduced premotoric processing time? Psychophysiology 41:231–244.
Joos K, Gilles A, Van de Heyning P, De Ridder D, Vanneste S (2014) From sensation to percept: the neural signature of auditory event-related potentials. Neurosci Biobehav Rev 42:148–156.
Kang MS, Diraddo A, Logan GD, Woodman GF (2014) Electrophysiological evidence for preparatory reconfiguration before voluntary task switches but not cued task switches. Psychon Bull Rev 21:454–461.
Krigolson OE, Holroyd CB, Van Gyn G, Heath M (2008) Electroencephalographic correlates of target and outcome errors. Exp Brain Res 190:401–411.
Krigolson O, Bell J, Kent CM, Heath M, Holroyd CB (2012) Reduced cortical motor potentials underlie reductions in memory-guided reaching performance. Mot Control 16:353–370.
Kutas M, Donchin E (1980) Preparation to respond as manifested by movement-related brain potentials. Brain Res 202:95–115.
Lakens D (2013) Calculating and reporting effect sizes to facilitate cumulative science: a practical primer for t-tests and ANOVAs. Frontiers Psychol 4.
Lamarche M, Louvel J, Buser P, Rektor I (1995) Intracerebral recordings of slow potentials in a contingent negative variation paradigm: an exploration in epileptic patients. Electroencephalogr Clin Neurophysiol 95:268–276.
Leuthold H, Sommer W, Ulrich R (1996) Partial advance information and response preparation: inferences from the lateralized readiness potential. J Exp Psychol Gen 125:307–323.
Loftus GR, Masson ME (1994) Using confidence intervals in within-subject designs. Psychon Bull Rev 1:476–490.
Loveless NE, Sanford AJ (1974) Slow potential correlates of preparatory set. Biol Psychol 1:303–314.
Luck SJ (2014) An introduction to the event-related brain potential technique. second ed. London: The MIT Press.
Luck SJ, Hillyard SA (1995) The role of attention in feature detection and conjunction discrimination: an electrophysiological analysis. Intl J Neurosci 80:281–297.
Mangun GR (1995) Neural mechanisms of visual selective attention. Psychophysiology 32:4–18.
Maraj A, Heath M (2010) Antipointing: perception-based visual information renders an offline mode of control. Exp Brain Res 202:55–64.
Milivojevic B, Hamm JP, Corballis MC (2009) Hemispheric dominance for mental rotation: it is a matter of time. NeuroReport 20:1507–1512.
Moon SY, Barton JJ, Mikulski S, Polli FE, Cain MS, Vangel M, Hämäläinen MS, Manoach DS (2007) Where left becomes right: a magnetoencephalographic study of sensorimotor transformation for antisaccades. Neuroimage 36:1313–1323.
Neely KA, Heath M (2009) Visuomotor mental rotation: reaction time is not a function of the angle of rotation. Neurosci Lett 463:194–198.
Neely KA, Heath M (2010a) Visuomotor mental rotation: reaction time is determined by the complexity of the sensorimotor transformations mediating the response. Brain Res 1366: 129–140.
Neely KA, Heath M (2010b) Visuomotor mental rotation: the reaction time advantage for anti-pointing is not influenced by perceptual experience with the cardinal axes. Exp Brain Res 201:593–598.

Neely KA, Heath M (2011) The visuomotor mental rotation task: visuomotor transformation times are reduced for small and perceptually familiar angles. J Mot Behav 43:393–402.
Nieuwenhuis S, Aston-Jones G, Cohen JD (2005) Decision making, the P3, and the locus coeruleus–norepinephrine system. Psychol Bull 131:510.
Ofori E, Coombes SA, Vaillancourt DE (2015) 3D Cortical electrophysiology of ballistic upper limb movement in humans. Neuroimage 115:30–41.
Pedhazur EJ (1997) Multiple regression in behavioral research: explanation and prediction. third ed. Orlando: Harcourt Brace College Publishers.
Pellizzer G, Georgopoulos AP (1993) Common processing constraints for visuomotor and visual mental rotations. Exp Brain Res 93:165–172.
Peronnet F, Farah MJ (1989) Mental rotation: an event-related potential study with a validated mental rotation task. Brain Cogn 9:279–288.
Polich J (2007) Updating P300: an integrative theory of p3a and p3b. Clin Neurophysiol 118:2128–2148.
Richter W, Ugurbil K, Georgopoulos A, Kim S-G (1997) Time-resolved fMRI of mental rotation. NeuroReport 8:3697–3702.
Ritter W, Simson R, Vaughan HG (1983) Event-related potential correlates of two stages of information processing in physical and semantic discrimination tasks. Psychophysiology 20:168–179.
Rossetti Y, Revol P, McIntosh R, Pisella L, Rode G, Danckert J, Tilikete C, Dijkerman HC, Boisson D, Vighetto A, Michel F, Milner AD (2005) Visually guided reaching: bilateral posterior parietal lesions cause a switch from fast visuomotor to slow cognitive control. Neuropsychologia 43:162–177.
Shepard RN, Metzler J (1971) Mental rotation of three-dimensional objects. Science 171:701–703.
Ulrich R, Leuthold H, Sommer W (1998) Motor programming of response force and movement direction. Psychophysiology 35: 721–728.
Vogel EK, Luck SJ (2000) The visual N1 component as an index of a discrimination process. Psychophysiology 37:190–203.
Volcic R, Wijntjes MW, Kool EC, Kappers AM (2010) Cross-modal visuo-haptic mental rotation: comparing objects between senses. Exp Brain Res 203:621–627.
Walter WG, Cooper R, Aldridge VJ, McCallum WC, Winter AL (1964) Contingent negative variation: an electric sign of sensorimotor association and expectancy in the human brain. Nature 203: 380–384.
Weiler J, Heath M (2014) Oculomotor task switching: alternating from a nonstandard to a standard response yields the unidirectional prosaccade switch-cost. J Neurophysiol 112:2176–2184.
Wijers AA, Otten LJ, Feenstra S, Mulder G, Mulder LJ (1989) Brain potentials during selective attention, memory search, and mental rotation. Psychophysiology 26:452–467.
Zaepffel M, Brochier T (2012) Planning of visually guided reach-to-grasp movements: inference from reaction time and contingent negative variation (CNV). Psychophysiology 49: 17–30.
Zhang M, Barash S (2000) Neuronal switching of sensorimotor transformations for antisaccades. Nature 408:971–975.

(Accepted 9 October 2015)
(Available online 23 October 2015)